Analysis of ^{4,6,8}He+^{208}Pb elastic scattering at $E = 22$ MeV using various potentials

Awad A. Ibraheem
Physics Department, King Khalid University, Abha, Saudi Arabia.

Physics Department, Al-Azhar University, Assiut Branch, Assiut 71524, Egypt

Huda Al-Amri
Physics Department, King Khalid University, Abha, Saudi Arabia.

Received 18 February 2022; accepted 09 April 2022

Using phenomenological and microscopic potentials, the experimental angular distributions for the ^{4,6,8}He nuclei elastically scattered from a ^{208}Pb target at $E_{lab} = 22$ MeV are investigated. Both the modified version of CDM3Y6 interaction based on the inclusion of the rearrangement term (RT) and those obtained from the Sao Paulo Potentials are used for the microscopic potentials. The cluster folding potential for ^{6}He+^{208}Pb is calculated using the triton + triton cluster structure for ^{6}He. This analysis revealed that the real cluster folding potential strength must be reduced by about 90%. Using the extracted potentials, the total reaction cross sections were successfully reproduced.

Keywords: Density distributions; elastic scattering; optical potential; cluster folding; CDCC; Sao Paulo potential.

DOI: https://doi.org/10.31349/RevMexFis.68.051201

1. Introduction

Elastic scattering processes between two colliding nuclei still remain an important topic in nuclear physics studies. The scientific community has been attracted to ^{4,6,8}He because of its special aspects in scattering with heavy targets. The weakly bound nucleus ^{6}He has a broad neutron distribution and a low 2n-binding energy, which is well known[1-4]. These characteristics favor neutron transfer and breakup, and therefore should affect the angular distribution of elastic cross sections [5-9]. ^{8}He has more valence neutrons but is more tightly bound, with binding energies comparable for 1n and 2n systems, whereas ^{6}He favors two-neutron breakup. The elastic and reaction cross sections for collisions with heavy targets at Coulomb barrier energies are expected to reflect the differences between the two helium isotopes.

A. M. Sanchez-Bentez *et al* [5] analyzed data of elastic scattering of 6He+208Pb measured at laboratory energies of 14, 16, 18, and 22 MeV using phenomenological Woods Saxon form factors and optical model calculations. The dispersion relations that connect the real and imaginary parts of the optical potential were found to be consistent with the energy variation of the optical potential.

The goal of this research is to see how sensitive ^{4,6,8}He +^{208}Pb elastic scattering is to various phenomenological and semi-microscopic potentials [10-16]. Various models have been used to explain nuclear-particle interactions.

Some of these approaches include the double-folding model (DFM), the Woods–Saxon (WS) potential, and various variations of the WS potential. However, for analyzing experimental angular distributions of low-energy scattering of exotic nuclei on stable nuclei, the well-known double-folding (DF) model is the most widely used method. The phenomenological OM as well as the DF with the appropriate optimized parameter sets accurately reproduce the elastic scattering angular distributions for ^{4,6,8}He +^{208}Pb elastic scattering. We reanalyzed the experimental data of the ^{4,6,8}He +^{208}Pb reaction at 22 MeV [8-16] by calculating the nuclear potential using a variety of potentials, including Sao Paulo potentials, CDM3Y6 potentials with and without the rearrangement term (RT), and phenomenological WS potentials [17-22].

The paper is organized as follows. Section 2 discusses the nuclear potentials that are used in the data analysis, while Sec. 3 discusses the results and discussion. The summary is provided in Sec. 4.

2. Theoretical methods

As a first step for probing the interaction mechanism for the considered nuclear systems, OM of the nucleus is applied. The implemented phenomenological OM potential has the following form:

$$U(r) = V_{\rm C} - V_0 \left[1 + \exp\left(\frac{r - R_V}{a_V}\right)\right]^{-1} - iW_0 \left[1 + \exp\left(\frac{r - R_W}{a_W}\right)\right]^{-1}. \quad (1)$$

The $V_C(r)$ is the Coulomb potential due to a uniform sphere with a charge equal to that of the target nucleus and radius $r_C\ A_t^{1/3}$.The nuclear potential is consisting from two parts: real volume (which simulate the scattering) and imaginary volume (simulate the reduction in flux due to absorption), both has the phenomenological Woods-Saxon (WS) shape.

According to the different parameter ambiguities both discrete and continuous associated with the OM calculations, and the fact that phenomenological representations do not include a description of the projectile or target's structure, the real part of potential was constructed using the microscopic double folding (DF) procedure extracted from the CDM3Y6 interactions with and without rearrangement term RT as well as Sao Paulo potential (SPP) via the double convolution integral

$$V_{DF}(r) = \iint \rho_p(r_1)\rho_t(r_2)v_{NN}(S)d^3r_1d^3r_2, \quad (2)$$

where $\rho_p(r_1)$, $\rho_t(r_2)$are the matter densities of the projectile and the target respectively and $v_{NN}(S)$is the effective *NN* interaction between two nucleons where $S = \overrightarrow{R} - \overrightarrow{r_1} + \overrightarrow{r_2}$. For *NN* effective interactions, the widely held choosing has been based on the M3Y interactions which were designed to reproduce the G-matrix elements of Paris [18-20] *NN* interactions. The density distribution of ^{4,6,8}He is deduced using the Argonne v18 two-nucleon and Urbana X three-nucleon potentials (AV18+UX) in a realistic Variational Monte Carlo (VMC) wave function [26]. For the density distributions of ^{208}Pb, the following fermi form is assumed [27,28].

$$\rho(r) = \frac{\rho_0}{1+\exp(r-R)/a}, \quad (3)$$

$R = 6.8\ fm\ , a = 0.515\ fm$ and root-mean-square (rms) matter radius of $5.604\ \ fm$, respectively while ρ_0 can be determined from the normalization condition.

$$4\pi \int \rho(r)\, r^2 dr = 208.0. \quad (4)$$

The DF potential consists mainly of two parts:

The direct part is

$$v_D(r) = \left[11062\frac{e^{-4r}}{4r} - 2538\frac{e^{-2.5r}}{2.5r}\right]\ \text{MeV}, \quad (5)$$

and the knock-on exchange part in the infinite-range exchange is

$$v_{Ex}(r) = \Bigg[-1524\frac{e^{-4r}}{4r} - 518.8\frac{e^{-2.5r}}{2.5r} - 7.847\frac{e^{-0.7072r}}{0.7072r}\Bigg]. \quad (6)$$

In this study, a modified version of the CDM3Y6 interaction is used, which includes the rearrangement term (RT) (CDM3Y6-RT). The density-dependent version (CDM3Y6) of the M3Y effective NN interaction based on the G-matrix elements of the Paris potential is used for the direct and exchange terms in Eqs. (5) and (6). [21], which is the full CDM3Y6 interaction form.

$$v_{D(Ex)}(\rho, r) = g(E)F(\rho)v_{D(Ex)}(r), \quad (7)$$

where, the density dependent function *F* is written as [21]

$$F(\rho) = 0.2658\ [1 + 3.8033\exp(-1.41\rho)\ - 4.0\rho], \quad (8)$$

and $g(E)$ is the additional energy dependent factor written as [21],

$$g(E) = \left[1 - 0.003\left(\frac{E}{A}\right)\right]. \quad (9)$$

The term $\Delta F(\rho)$ is added to the folding model calculation for the modified (CDM3Y6-RT) interaction with the inclusion of the RT term, where $\Delta F(\rho)$ can be written as [29],

$$\Delta F(\rho) = 1.5\,[\exp(-0.833\rho) - 1]. \quad (10)$$

In the SPP model, the following two equations link the real part of the local-equivalent interaction to the DF potential $V_F(R)$as

$$V_F(R) = \iint \rho_{\mathrm{P}}(\mathrm{r_P})\,\rho_{\mathrm{T}}(\mathrm{r_T})\,V_0\delta\left(\left|\overrightarrow{\mathrm{s}}\right|\right)\mathrm{d}^3\mathrm{r_P}\mathrm{d}^3\mathrm{r_T},$$
$$\overrightarrow{\mathrm{s}} = \overrightarrow{\mathrm{R}} - \overrightarrow{\mathrm{r}}_{\mathrm{P}} + \overrightarrow{\mathrm{r}}_{\mathrm{T}}, \quad (11)$$

where $\rho_{\mathrm{P}}(\mathrm{r_P})$ and $\rho_{\mathrm{T}}(\mathrm{r_T})$, respectively are the nuclear matter density distributions for the two colliding nuclei. The following two equations link the real part of the local-equivalent interaction to the DF potential $V_F(R)$as

$$V_N(R,E) = V_F(R)\ \exp\left(-\left[\frac{2v}{c}\right]^2\right), \quad (12)$$

$$V^2(R,E) = \frac{2}{\mu}(E - V_C(R) - V_N(R,E)). \quad (13)$$

Where *V* is the nuclei's local relative velocity and C is the speed of light. The nuclear densities were obtained from the Dirac-Hartree-Bogoliubov model [30], and the Sao Paulo potential (SPP2) was calculated using the REGINA code [20].

3. Results and discussion

For incident energies of $E_{lab} = 22$ MeV, elastic scattering results for the ^{4,6,8}He + ^{208}Pb reactions were obtained. Three different theoretical approaches were used for this purpose microscopic double folding model based on Sao Paulo potential, CDM3Y6 interaction with and without RT, and phenomenological Woods Saxon (WS) model. The potentials that resulted are represented in Fig. 1. The comparisons between the experimental ^{4,6,8}He nuclei elastically scattered from a ^{208}Pb target at $E = 22$ MeV and the theoretical calculations using both phenomenological OM and microscopic model are shown in the Fig. 2.

For the real and imaginary potentials, three parameters were used in the OM computations. Depths, radius, and diffuseness for the real (v_0, r_0, a_0) and imaginary (w_0, r_w, a_w) volume parts of the interaction potential were freely changed

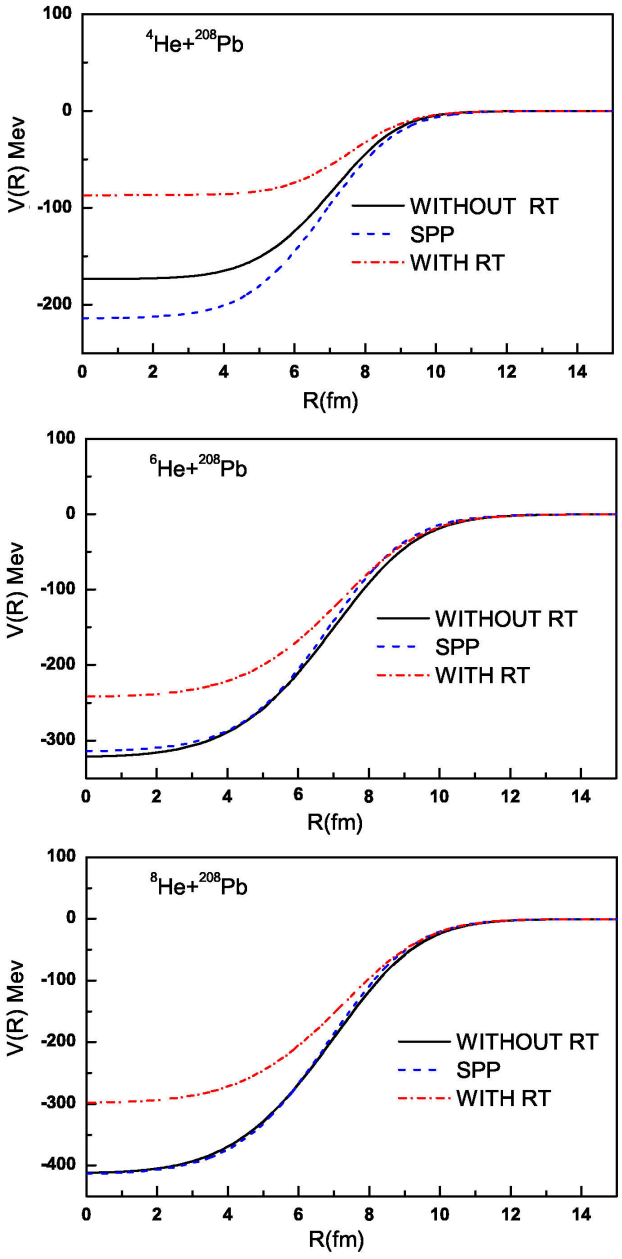

FIGURE 1. The generated real SPP as well as CDM3Y6 with and without RT for ^{4,6,8}He + ^{208}Pb target at $E_{lab} = 22$ MeV.

until the best fit for the data was achieved by minimizing the χ^2 value defined by

$$\chi^2 = \frac{1}{N}\sum_{i=1}^{N}\left(\frac{\sigma(\theta_i)^{\rm cal} - \sigma(\theta_i)^{\rm exp}}{\Delta\sigma(\theta_i)}\right)^2, \qquad (14)$$

where N is the number of data points, $\sigma(\theta_i)^{\rm cal}$ and $\sigma(\theta_i)^{\rm exp}$ are the calculated and experimental differential cross sections (DCs) and $\Delta\sigma(\theta_i)$is the relative uncertainty in experimental data.

The parameters with the best fit are listed in the table. The theoretical fits were done with the FRESCO code [27], and the optimal potential parameters were found with the SFRESCO search code. For the ^{6,8}He, it is obvious that the

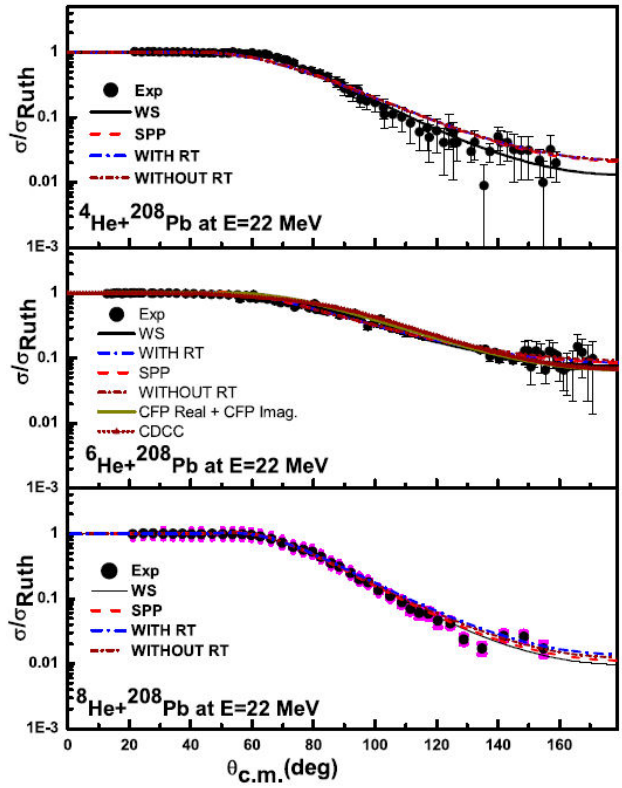

FIGURE 2. Comparison of experimental angular distributions (solid black circles) and theoretical calculations (solid red curves) for ^{4,6,8}He+^{208}Pb elastic scattering using WS and real folded potential at E_{lab}= 22 MeV. Ref.[10-16] provided the experimental data. Cluster folding potential for ^{6}He+^{208}Pb is performed by considering triton + triton cluster structure for ^{6}He as well as the CDCC calculations.

agreement between theoretical results and experimental data is almost perfect. The results of the ^{4}He+^{208}Pb reaction, in particular, are shown to be almost excellent for the WS model, which properly represents the experimental data for both small and large angles. However, the conclusions of the SPP and CDM3Y6 models for all incidence energy exclude some angles of the experimental data.

For each reaction, we calculated volume integrals as well as chi square χ^2 values. Using various versions of the nuclear model of the ^{4,6,8}He nucleus, we found that the phenomenological potential (WS) with 6-free parameters provides good fitting for all systems, as evidenced by the chi square values in Table I, whereas the other microscopic potentials, the obtained values for the chi square value give a closed value to each other. Real real (J_R) and imaginary (J_I) volume integrals are used to calculate the volume integral. The J_R and J_I volume integrals are crucial for demonstrating the evaluated potential's strength. In this context, the Table shows the J_R and J_I values for the WS, SPP, and CDM3Y6 models. It has been found that altering the used model results in similar J_R and J_R values. The smallest values for the WS results can be seen when the χ^2 values are examined. Of course, a lower chi square χ^2 value corresponds to a more accurate description

TABLE I. The Optical potential parameters obtained from analysis of the ^{4,6,8}He + ^{208}Pb elastic scattering at $E = 22$ MeV using WS, folded potential based on CDM3Y6 with and without rearrangement term, Sao Paulo potential (SPP), as well as cluster folding potential (CFP). Volume depth (V_0 ,W_0), radius and diffuseness parameters (r_i, a_i), $i = v, w$. "Real and imaginary volume integrals (J_R and J_I), total reaction cross section (σR) and the best fit $\chi 2$ are presented.

Model	**V(N_r)**	$\mathbf{r}_V$	$\boldsymbol{a}_V$	**W**	$\mathbf{r}_W$	$\boldsymbol{a}_W$	$\boldsymbol{\chi^2/N}$	σ_R	$\mathbf{J}_R$	$\mathbf{J}_I$
^{4}He+^{208}Pb										
WS	9.442	1.850	0.850	9.11	1.850	0.7932	0.759	1255	66.32	63.52
SPP	1.0			6.178	1.850	1.306	1.688	1661	399.29	46.46
RT	1.0			7.319	1.850	1.2658	1.972	1693	196.32	54.86
RT=0	0.95			7.303	1.850	1.266	1.984	1693	335.68	54.74
^{6}He+^{208}Pb										
WS	23.72	1.4817	0.8501	139.99	1.850	0.300	3.05	1159	88.28	935.06
SPP	0.996			139.62	1.5949	0.850	2.543	1280	400.1	640.53
RT	0.998			39.365	1.850	0.7382	2.822	1333	350.89	272.69
RT=0	0.995			39.205	1.850	0.7420	2.835	1340	430.47	271.70
CFP	0.1			3.0			3.0	1330	43.2	187.4
^{8}He+^{208}Pb										
WS	17.15	1.5456	0.850	139.91	1.850	0.6506	5.33	1461	71.94	959.92
SPP	0.95			137.95	1.5834	0.7975	7.13	1408	286.75	614.38
RT	1.0			149.99	1.5834	0.7975	7.74	1412	326.30	668.01
RT=0	1.06			149.99	1.5834	0.7975	6.84	1420	439.12	668.01

description of the experimental data in terms of the chosen theoretical representation. As a result, similar cross sections for various approaches can indicate similar experimental results [6-12]. As a result, it is reasonable to assume that various approaches have resulted in a successful analysis of the experimental data.

To validate our analysis, we plotted expression (12) at 22 MeV for ^{4,6,8}He+^{208}Pb and, against the DF potential with finite-range exchange contribution for the densities under consideration, as shown in Fig. 1. At the center (R=0), $(V^{SPP}(0)/V^{DF}(0))\approx 1.2)(0.98(1.01))$ for ^{4}He,^{6}He and ^{8}He respectively without RT, this means that the scattering is sensitive to the real potential for both reactions considered. This figure shows that the DF potential is about 5% deeper than the SPP potential at the center ($R = 0$), while they are similar for radial distances R ranging from 0.5 fm to 7 fm for ^{6,8}He+^{208}Pb scattering.

A strong absorption radius R_S (closest approach) through the surface radial region can be defined as the distance between colliding particles in terms of the transmission coefficient $T_{1/2}$, which is a function of the partial wave and momentum L1/2, as well as the Sommerfield parameter η and the projectile wave number k [28]. We can see that the different DF and cluster potentials agree with each other near the strong absorption radius R_S where $R_S = 10.5$, 10.8, 11.1 fm for the ^{4,6,8}He+^{208}Pb reaction.

3.1. Cluster folding Potential for ^{6}He+^{208}Pb

Cluster folding (CF) potential obtained from the t + t probable cluster structure for $6_{\mathrm{He}} + 208_{\mathrm{Pb}}$ elastic scattering data is used to fit the data. Based on the suggested t + t model, the real and imaginary CF potentials for ^{6}He + ^{208}Pb system can be defined on the basis of t + ^{208}Pb potentials as: the real and imaginary CF potentials for the ^{6}He + ^{208}Pb system may be defined on the basis of $t + t$ model. Using the recommended $t+t$ model as follows, we can write the ^{6}He + ^{208}Pb potential as

$$V^{CF}(R) = \int [V_{t-^{208}\mathrm{Pb}}(\mathbf{R} - \frac{1}{2}\mathbf{r}) + V_{t-^{208}\mathrm{Pb}}(\mathbf{R} + \frac{1}{2}\mathbf{r})]|\chi_{t-t}(\mathbf{r})|^2 \mathrm{d}\mathbf{r}. \quad (15)$$

The $V_{t-\,^{208}\,\mathrm{Pb}}$ is the phenomenological potential for the two t + ^{208}Pb channels which fairly reproduce the experimental data at the appropriate energies $E_t \approx 1/2E(^6_{He})$ taken from [29]. The term $\chi_{t-t}(\mathbf{r})$ is the intercluster wave function for the relative motion of the two tritons in the ground state of ^{6}He, and $\mathbf{r}$ is the relative coordinate between the centers of mass of two tritons. The bound state form factor $t + t$ represents a $2S_{1/2}$ state in a real Woods-Saxon potential of $R = 1.15$ fm, $a = 0.7$ fm, and the potential depth is allowed to be changed till reach the binding energy of the cluster (12.307 MeV). The constructed cluster folding potential for ^{6}He + ^{208}Pb is shown in Fig. 3.

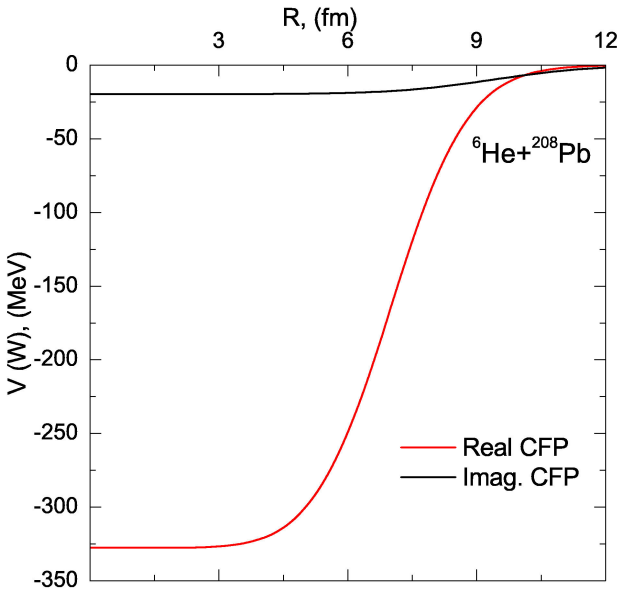

FIGURE 3. Real cluster folding potential used in ^{6}He+^{208}Pb analysis at $E = 22$ MeV.

The ^{6}He + ^{208}Pb experimental angular distribution at $E = 22$ MeV "see Fig. 2" is reanalyzed within the framework of cluster folding model using two adjustable parameters N_{RCF} and N_{ICF}, namely the renormalization factor for the real and imaginary cluster folding potentials, respectively, derived based on Eq. (14) and presented in Fig. 1. The analysis showed the necessity to reduce the real cluster folding potential strength by about 90%. Although, it is well known that, in order to fit the experimental cross sections for systems induced by weakly projectiles such as ^{6,7}Li and ^{6}He, the potential strength should be reduced by $\sim$ 40-60 % [30-35], the reported reduction (90%) in the potential strength could infer the less probability of ^{6}He to be treated as a cluster of two tritons. More sophisticated approaches could be preferable to derive the interaction potential based on three body treatment (^{4}He+n+n) for ^{6}He. Generally, the adopted potentials either Woods-Saxon or double folded CDM3Y6 potentials with and without considering the rearrangement term fairly described the considered data for ^{4,6,8}He scattered from ^{208}Pb at $E = 22$ MeV, where the extracted N_r is very close to unity.

The Continuum discretized coupled channels (CDCC) were used to investigate a three-body projectile ^{6}He (n+n+^{4}He), assuming that the two neutrons are di-neutrons and thus take the shape of a two-body projectile (^{6}He+2n). Moro *et al.* [40] improved this di-neutron model to account for four-body effects by using an effective di-neutron separation energy, they observed an effective binding energy of around 1.6 MeV rather than the 0.973 MeV predicted in the previous model [40-42]. To investigate the effect of couplings to the breakup channels, the (CDCC) method is used to analyze the experimental elastic scattering angular distributions for ^{6}He+^{208}Pb at $E = 22$ MeV. The results of the differential cross section using CDCC and other models are compared in Fig. 2. The total reaction cross section calculated by CDCC is equal 1313.4 mb, which agrees with the results of the other microscopic models.

4. Summary

The current study's main goal is to conduct a further analysis of the interaction mechanism and peculiarities resulting from the scattering of ^{4,6,8}He from the heavy target ^{208}Pb at energy $E = 22$ MeV, above the Coulomb barrier. Analysis performed within both the derived real potential and the phenomenological WS potential. The DF potentials with CDM3Y6 effective interaction is considered with and without taking into consideration the effect of rearrangement term as well as Sao Paulo calculations. For ^{4,6,8}He+^{208}Pb nuclear system, the strength of the real double folded part is closed to unity to reproduce the data. All of the results are compared to the experimental data as well as to each other. On the other hand, due to the lower probability of ^{6}He being treated as a cluster of two tritons, the analysis revealed the need to reduce the real cluster folding potential strength by approximately 90%. Additionally, for each theoretical approach, we provide potential parameters, cross sections, volume integrals, and chi square values. The calculated potential's renormalization factor is maintained near unity. At all angular regions where the real part of potential plays a critical role in cross section calculations, the agreement between experimental data and calculated cross sections using folded potential is fairly good.

Acknowledgement

H. Alamri is gratefully acknowledge to King Abdul-Aziz City for Sciences and Technology (KACST), Kingdom of Saudi Arabia for their financial support provided through project (1-17-01-010-0025) .

1. I. Tanihata, H. Savajols and R. Kanungo, *Recent experimental progress in nuclear halo structure studies*, Progress in Particle and Nuclear Physics **A68** (2013) 215, https://doi.org/10.1016/j.ppnp.2012.07.001.

2. G. D. Alkhazov *et al.*, *Nuclear matter distributions in the ^{6}He and ^{8}He nuclei from differential cross sections for small-angle proton elastic scattering at intermediate energy*, Nuclear Physics **A712** (2002) 269, https://doi.org/10.1016/S0375-9474(02)01273-3.

3. M. C. Parker, C. Jeynes and W. N. Catford, *Halo Properties in Helium Nuclei from the Perspective of Geometrical Thermo-*

dynamics, Annalen der Physik **534** (2022) 2270003, https://doi.org/10.1002/andp.202270003.

4. M. Aygun, Y. Kucuk, I. Boztosun and A. Ibraheem, *Microscopic few-body and Gaussian-shaped density distributions for the analysis of the ^{6}He exotic nucleus with different target nuclei*, Nuclear Physics A **848** (2010) 245, https://doi.org/10.1016/j.nuclphysa.2010.09.005.

5. A. M. Snchez-Bentez *et al.*, *Study of the elastic scattering of ^{6}He on ^{208}Pb at energies around the Coulomb barrier*, Nuclear Physics **A803** (2008) 30, https://doi.org/10.1016/j.nuclphysa.2008.01.030.

6. G. Marquínez-Durn *et al.*, *ELASTIC SCATTERING OF 8He + 208Pb AT 22 MeV*, ACTA PHYSICA POLONICA **B 44** (2013) 467, https://doi.org/10.5506/APhysPolB.44.467.

7. L. Acosta *et al.*, *Elastic scattering and α-particle production in ^{6}He + ^{208}Pb collisions at 22 MeV*, Phys. Rev. **C 84** (2011) 044604. https://doi.org/10.1103/PhysRevC.84.044604.

8. D. Escrig *et al.*, *particle production in the scattering of ^{6}He by ^{208}Pb at energies around the Coulomb barrier*, Nucl. Phys. **A 792** (2007) 2, https://doi.org/10.1016/j.nuclphysa.2007.05.012.

9. Awad A. Ibraheem and M. Aygun, *Optical model analysis of alpha particle scattering*, Indian Journal of Physics *95* (2021) 2437, https://doi.org/10.1007/s12648-020-01903-3.

10. A. M. Sánchez-Benitez *et al.*, *Scattering of ^{6}He at energies around the Coulomb barrier*, Journal of Physics G: Nuclear and Particle Physics **31** (2005) S1953, https://doi.org/10.1088/0954-3899/31/10/109.

11. G. Marquínez-Durán *et al. Scatteing of ^{8}He on ^{208}Pb at energies round the Coulomb barrier*, Acta Physica Polonica B **43** (2012) 239, https://doi.org/10.5506/APhysPolB.43.239.

12. G. Marquínez-Durán *et al. Interaction of ^{8}He with ^{208}Pb at near-barrier energies: ^{4}He and ^{6}He production*, Phys. Rev. **C 98** (2018) 034615, https://doi.org/10.1103/PhysRevC.98.034615.

13. G. Marquínez-Durún *et al. Precise measurement of near-barrier ^{8}He+^{208}Pb elastic scattering: Comparison with ^{6}He*, Phys. Rev. **C 94** (2016) 064618, https://doi.org/10.1103/PhysRevC.94.064618.

14. R. Barnett and J. S. Lilley, *Interaction of alpha particles in the lead region near the Coulomb barrier*, Phys. Rev. **C9** (1974) 2010, https://doi.org/10.1103/PhysRevC.9.2010.

15. R. Barnett and J. S. Lilley, *Interaction of alpha particles in the lead region near the Coulomb barrier*, Phys. Rev. **C 9** (1974) 2010, https://doi.org/10.1103/PhysRevC.9.2010.

16. G.Goldring ,B.A.Watson,M. C.Bertin and S.L.Tabor ,*Alpha-particle scattering from ^{204,206,208}Pb and ^{209}Bi at incident energies near the coulomb barrier* Phys. Lett. B **32** (1970) 465, https://doi.org/10.1016/0370-2693(70)90385-0.

17. L. C. Chamon *et al.*, *Nonlocal Description of the Nucleus-Nucleus Interaction*, Phys. Rev. LETT. **79** (1997) 5218, https://doi.org/10.1103/PhysRevLett.79.5218.

18. L. C. Chamon, D. Pereira and M. S. Hussein,*Parameterfree account of quasielastic scattering of stable and radioactive nuclei*, Phys. Rev. **C 58** (1998) 576, https://doi.org/10.1103/PhysRevC.58.576.

19. L. C. Chamon,*The S?o Paulo Potential*, Nucl. Phys. **A 787** (2007) 198c. https://doi.org/10.1016/j.nuclphysa.2006.12.032.

20. L. C. Chamon, B. V. Carlson and L. R. Gasques,*Sao Paulo potential version 2 (SPP2) and Brazilian nuclear potential (BNP)*, Comp. Phys. Comm.**267** (2021) 108061. https://doi.org/10.1016/j.cpc.2021.108061.

21. D. T. Khoa, G. R. Satchler and W. von Oertzen, *Nuclear incompressibility and density dependent NN interactions in the folding model for nucleus-nucleus potentials*, Phys. Rev. **C 56** (1997) 954. https://doi.org/10.1103/PhysRevC.56.954.

22. D. T. Khoa, *α-nucleus optical potential in the double-folding model* Phys. Rev. C **63** (2001) 034007, https://doi.org/10.1103/PhysRevC.63.034007.

23. Bertsch G F, Borysowicz J, Mcmanus H and Ae W G,*Interactions for inelastic scattering derived from realistic potentials*, Nucl. Phys. A **284** (1977) 399, https://dx.doi.org/10.1016/0375-9474(77)90392-X.

24. Anantaraman N, Toki H and Bertsch G F,*An effective interaction for inelastic scattering derived from the Paris potential*, Nucl. Phys. A **398** (1983) 269. https://doi.org/10.1016/0375-9474(83)90487-6.

25. M. El-Azab Farid and G. R. Satchler, *A density-dependent interaction in the folding model for heavy-ion potentials*, Nucl. Phys. A **438** (1985) 525, https://doi.org/10.1016/0375-9474(85)90391-4.

26. https://www.phy.anl.gov/theory/research/density/.

27. R.E. Warner *et al.*,*Total reaction and 2n-removal cross sections of 20–80A MeV ^{4,6,8}He , $^{6-9,11}$Li, and ^{10} Be on Si*, Phys. Rev. C**54** (1996) 1700. https://link.aps.org/doi/10.1103/PhysRevC.54.1700.

28. M. El-Azab Farid and M. A. Hassanain,Density-independent folding analysis of the ^{6,7}Li elastic scattering at intermediate energies, Nucl. Phys. A **678** (2000) 39, https://doi.org/10.1016/S0375-9474(00)00313-4.

29. D. T. Khoa, N. Hoang Phuc, D. Thi Loan and B. Minh Loc, *Nuclear mean field and double-folding model of the nucleus-nucleus optical potential*, Phys. Rev. C **94** (2016) 034612, https://link.aps.org/doi/10.1103/PhysRevC.94.034612.

30. B. V. Carlson and D. Hirata,*Dirac-Hartree-Bogoliubov approximation for finite nuclei*, Phys. Rev. C **62** (2000) 054310, https://doi.org/10.1103/PhysRevC.62.054310.

31. I. J. Thompson, *Coupled reaction channels calculations in nuclear physics*,Comput. Phys. Rep. **7** (1988) 167, https://doi.org/10.1016/0167-7977(88)90005-6.

32. G. R. Satchler and W. G. Love,*Folding model potentials from realistic interactions for heavy-ion scattering*, phys. Rep. **55** (1979) 183, https://doi.org/10.1016/0370-1573(79)90081-4.

33. R. A. Hardekopf, L. R. Veeser and P. W. Keaton Jr.,*Polarization Measurements and Optical-Model Potential for Tritons*, Phys. Rev. Lett. **35** (1975) 1623, https://doi.org/10.1103/PhysRevLett.35.1623.

34. Sh. Hamada and Awad A. Ibraheem,*Peculiarities of ^{6}Li+^{12}C elastic scattering*, Int. J. Mod. Phys. E **28** (2019) 1950108. https://doi.org/10.1142/S0218301319501088.

35. Sh. Hamada *et al.*, *Analysis of ^{6}Li+^{16}O elastic scattering using different potentials, Rev. Mex. Fis.* **66** (2020) 322. https://doi.org/10.31349/RevMexFis.66.322.

36. Sh. Hamada and Awad A. Ibraheem,*Cluster folding optical potential analysis for ^{6}Li+^{28}Si elastic scattering*, Revista Mexicana de Fisica **67** (2021) 276. https://doi.org/10.31349/RevMexFis.67.276.

37. Sh. Hamada, Norah A. M. Alsaif and Awad A. Ibraheem,*Detailed analysis for ^{6}Li+^{40}Ca elastic scattering using different potentials*, Phys. Scr. **96** (2021) 055306, https://doi.org/10.1088/1402-4896/abeba6.

38. Awad A. Ibraheem *et al.*,*Elastic and Inelastic Scattering of 9,10,11Be by 64Zn and 120Sn Nuclei at Different Energies*, Braz. J. Phys. **753** (2021) 51. https://doi.org/10.1007/s13538-020-00839-7.

39. Awad A. Ibraheem, N. A. M. Alsaif, M. Al-Ahmari and Sh. Hamada,*Further investigation of $^{10,11}B$ + ^{58}Ni elastic scattering* , Phys. Scr. **96** (2021) 115307, https://doi.org/10.1088/1402-4896/ac183f.

40. A. M. Moro Muñoz, K. M. Rusek, J. M. Arias Carrasco, J. J. Gómez Camacho, M. Rodríguez Gallardo, *Improved di-neutron cluster model for 6He scattering*, Phys. Rev. C **75** (2007) 064607. https://doi.org/10.1103/PhysRevC.75.064607.

41. N. Keeley,*et al., Effect of E1 excitations to the continuum: 6He and 6Li+209Bi compared* Phys. Rev.C **68** (2003) 054601. https://doi.org/10.1103/PhysRevC.68.054601.

42. E.F. Aguilera *et al., Transfer and/or Breakup Modes in the 6He+209Bi Reaction near the Coulomb Barrier,* Phys. Rev. Lett. **84** (2000) 5058. https://doi.org/10.1103/PhysRevLett.84.5058.